JOURNAL OF PROPULSION AND POWER
Vol. 22, No. 1, January–February 2006

Technical Notes

TECHNICAL NOTES are short manuscripts describing new developments or important results of a preliminary nature. These Notes should not exceed 2500 words (where a figure or table counts as 200 words). Following informal review by the Editors, they may be published within a few months of the date of receipt. Style requirements are the same as for regular contributions (see inside back cover).

Fourier Modeling of Steady and Unsteady Nonaxisymmetrical Flows

L. He*
Durham University,
Durham, England DH1 3LE, United Kingdom

I. Introduction

In general, nonlinear flow disturbances in time and/or space can be identified and represented by a discrete Fourier series as long as they are periodic. For most engineering applications, only a few lower-order harmonics will be sufficient. The method of using the Fourier series in computing nonlinear time-domain unsteady flows in turbomachinery has been firstly proposed by He.[1] Development and applications of the Fourier transform type of phase-shift condition have been progressed for rotor-stator blade row aerodynamic interactions,[2–4] inlet distortions,[5] and aeroacoustic propagations in ducted fans.[6] Recently efficient Fourier-transform-based solution methods have been developed by Hall et al.[7] and McMullen et al.[8] for periodic unsteady flows.

The present work is aimed at extending the Fourier modeling methodology to nonaxisymmetrical steady and unsteady flows, in conjunction with the technique of a simultaneous Fourier transform.[7] The utility/applicability is of general relevance to aerodynamics and aeroacoustics of duct flows subject to circumferential distortions. It is also relevant to turbomachinery aeroelasticity, as flutter behavior of both frontal fan and last stage low-pressure turbine blades can be considerably influenced by upstream/downstream ducting. These ducting configurations are typically of much longer length scales compared to that of a blade passage and often subject to nonaxisymmetrical flow and/or geometrical conditions.

II. Modeling of Nonaxisymmetrical Steady Flow

A. Model Formulation

Consider a circumferential nonuniform flow with a wavelength of the whole circumference. Taking a cylindrical coordinate system (x, r, θ), we approximate the circumferential variation by the Nth-order discrete Fourier series, thus

$$U(x, r, \theta) = \bar{U}(x, r) + \sum_{n=1}^{N} [A_n \sin(n\theta) + B_n \cos(n\theta)] \qquad (1)$$

where $\bar{U}$ is the circumferentially averaged value of flow variable U. The Fourier coefficients An and Bn only depend on the axial and radial coordinates (x, r).

Presented as Paper 2005-0016 at the AIAA 43rd Aerospace Sciences Meeting and Exhibit, Reno, 10–13 January 2005; received 22 January 2005; revision received 10 August 2005; accepted for publication 28 June 2005.

*Professor and Chairman, Thermodynamics and Fluid Mechanics, School of Engineering; Li.He@durham.ac.uk.

The purpose of using the Fourier approximation is to reduce the computing resource required by a direct calculation of the whole domain of 360-deg circumference. The circumferential domain can be truncated to such an extent as long as it can provide sufficient information to carry out the Fourier transform. The minimum requirement for an Nth-order Fourier series would be $2N + 1$ points evenly spaced over the circumference. For instance, three circumferential mesh cells would be sufficiently needed for the Fourier transform if only one harmonic is retained (Fig. 1). In general, $2N + 1$ mesh cells will be placed in the following circumferential positions for an Nth-order Fourier series:

$$\theta_i = [i/(2N + 1)]2\pi \qquad (i = 1, 2, \ldots, 2N + 1) \qquad (2)$$

Now effectively we only have $2N + 1$ circumferential discrete mesh cells.

Consider that the flow equations are discretized by a typical cell-centered finite volume scheme and solved by an explicit time-marching integration. After each step of the time-marching integration, the flow variables at cell centers of the $2N + 1$ mesh cells have been updated. These at the $2N + 1$ cell centers are then used to carry out the circumferential Fourier transform, giving the Fourier coefficients:

$$A_n(x, r) = \frac{2}{2N + 1} \sum_{i=1}^{2N+1} U_i \sin(n\theta_i) \qquad (3a)$$

$$B_n(x, r) = \frac{2}{2N + 1} \sum_{i=1}^{2N+1} U_i \cos(n\theta_i) \qquad (n = 1, 2, \ldots, N) \qquad (3b)$$

The resultant Fourier series gives the simultaneous and complete circumferential flow distribution. Next we have to consider how to evaluate/assign the flow variables at the dummy points to enable fluxes or differences calculations. In this case, the values at the circumferential dummy points are given by the Fourier series with corresponding phase shifts. If the phase for the cell center is θ_i, the values at the two dummy points (Fig. 2) are then simply determined by

$$U(x, r, \theta_i + \Delta\theta) = \bar{U}(x, r) + \sum_{n=1}^{N} \{A_n \sin[n(\theta_i + \Delta\theta)] + B_n \cos[n(\theta_i + \Delta\theta)]\} \qquad (4a)$$

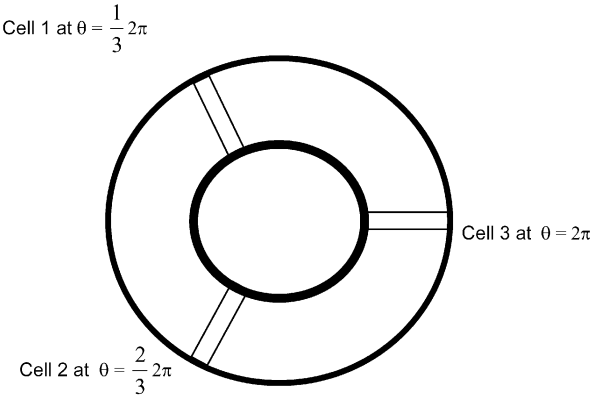

Fig. 1 Computational mesh cells required for one Fourier harmonic ($N = 1$).

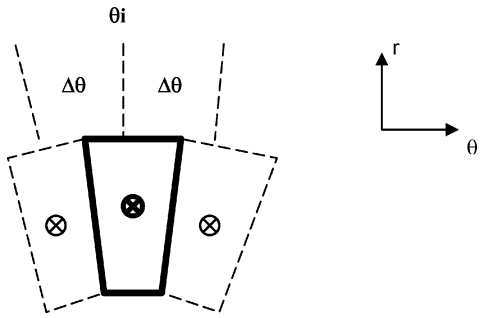

Fig. 2 Computational cell and its circumferential dummy points.

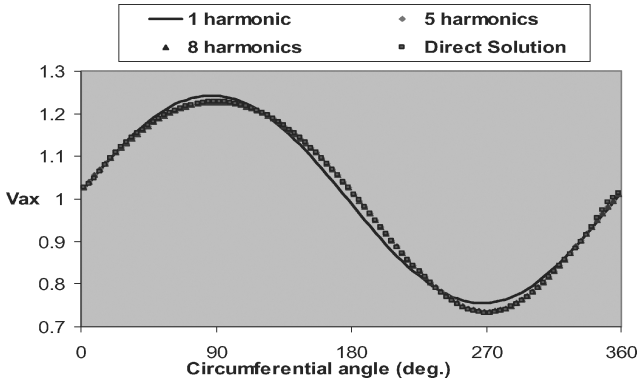

Fig. 3 Circumferential distributions of axial velocity at duct domain exit (inlet distortion of 50% dynamic head).

$$U(x, r, \theta_i - \Delta\theta) = \bar{U}(x, r) + \sum_{n=1}^{N} \{A_n \sin[n(\theta_i - \Delta\theta)] + B_n \cos[n(\theta_i - \Delta\theta)]\} \tag{4b}$$

Once the values at the dummy points are determined, fluxes/differences can be computed for the next step of iteration.

B. Computational Examples

The Fourier-transform-based method has been implemented in a multiblock structured-mesh Reynolds-averaged Navier–Stokes (RANS) solver. The governing equations are discretized with a cell-centered finite volume scheme and integrated in time using the explicit four-stage Runge–Kutta scheme. The Fourier transform and update are carried out at each fractional time-marching step.

First, a simple two-dimensional flow on the x–θ plane is considered. The full domain for a direct computation is between $x = 0$ and 0.5 m and between $\theta = 0$ and 360 deg, covered by 100 mesh points in the axial direction and 100 in the circumferential direction. The flow is subject to a stationary sinusoidal stagnation pressure distortion at the domain inlet. The amplitude of the stagnation pressure distortion is 5%, corresponding to 50% of the circumferentially averaged dynamic head. Five harmonics (hence 11 circumferential mesh cells) are used in the Fourier solution. The circumferential phase-shift relation enables a whole 360-deg domain flowfield to be constructed, which can be directly compared to the direct full domain solution. The axial-velocity distributions along the circumferential distance at the domain exit are given in Fig. 3. The axial-velocity distribution is not quite sinusoidal because of nonlinearity, and this nonlinear effect is adequately captured by the Fourier solution with three harmonics. A further increase in the number of harmonics retained leads to little difference. The results with five and eight harmonics are almost identical.

The second example is a three-dimensional annulus intake duct (inner radius of 0.2 m, outer radius of 0.8 m, axial length of 0.8 m) subject to a 10-deg crosswind. The computational mesh for the direct full-domain calculation is shown in Fig. 4, where 300 circumferential mesh cells cover the 360-deg whole annulus domain. At the inlet, circumferential distortions in the circumferential and

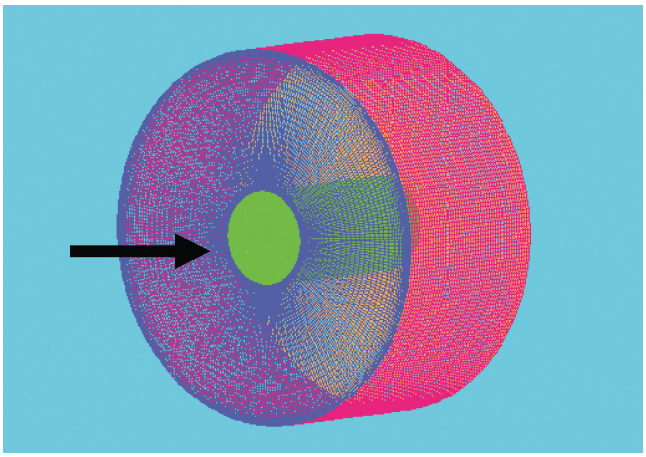

Fig. 4 Computational mesh for an annular duct.

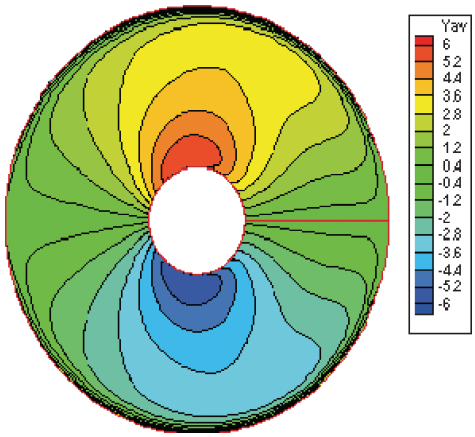

a) Fourier solution (11 mesh cells)

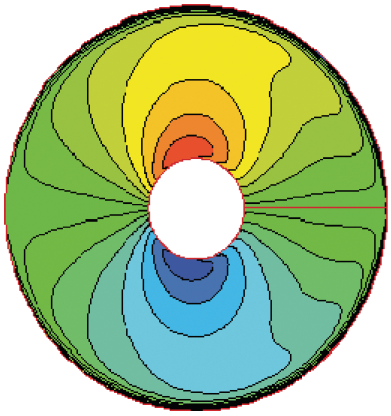

b) Direct solution (300 mesh cells)

Fig. 5 Circumferential flow angles (in degrees) at duct exit (10-deg crosswind from right to left at inlet).

radial inflow angles are specified. Both the circumferential and radial angle distortions are in a sinusoidal form with an amplitude of 10 deg. But the two angles are offset by a 90-deg circumferential phase difference. The radial angle distortion decays quickly through the duct, whereas the distortion in the circumferential flow angle is more persistent downstream (Fig. 5). The direct 360-deg domain calculation (300 circumferential mesh cells) is shown in Fig. 5b. The Fourier solution (Fig. 5a) retaining five harmonics needs only 11 circumferential mesh cells. Both solutions are in very good agreement, demonstrating the validity and implementation of the Fourier-transform-based method.

The next example is an outlet guide vanes (OGV) and pylon-combined configuration for aeroengines. The nonuniform potential

field with a wavelength of the whole annulus as generated by the pylon can propagate across the OGV and lead to aerodynamically and aeromechanically detrimental effects.[9] The whole flow domain has two very different length scales of interest: the nonuniform pylon field and the OGV blade passage. The OGV region requires a much higher mesh density and dominates the overall mesh requirement. In this example the Fourier modeling with the circumferential domain truncation is applied to the OGV region. It is recognized that for a bladed region the basic circumferentially truncated mesh domain will have to be one blade passage, whereas for a duct field the basic truncated domain contains only one mesh cell. Here, the OGV row has 30 cambered blades. The inlet flow (Mach number of 0.44) to OGV has a swirl angle of 30 deg. The OGV domain is truncated from 30 passages to five discrete passages, which are circumferentially evenly distributed for a Fourier solution with two harmonics. The computational mesh and static-pressure contours by the Fourier solution are shown in Fig. 6. Also carried out is a Fourier solution with one harmonic only (i.e., three discrete OGV passages meshed). The static-pressure distributions at the OGV inlet are plotted in Fig. 7 for the two Fourier solutions in comparison with a direct solution (30 OGV passages). It is noted from the direct solution that the circumferential pressure distribution is nonsinusoidal. The circumferential distance between the positive and negative peaks is only about 42% (instead of 50%) of the circumference. The Fourier solution with one harmonic does not capture this behavior, although the peak-peak nonuniform pressure magnitude is reasonably well predicted. The solution with two harmonics, however, gives a marked improvement and good agreement with the direct

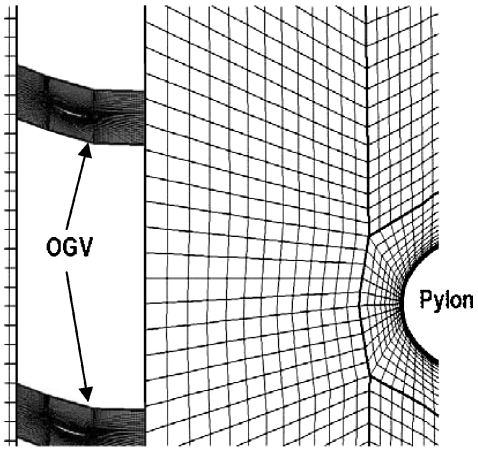

a) Mesh close-up

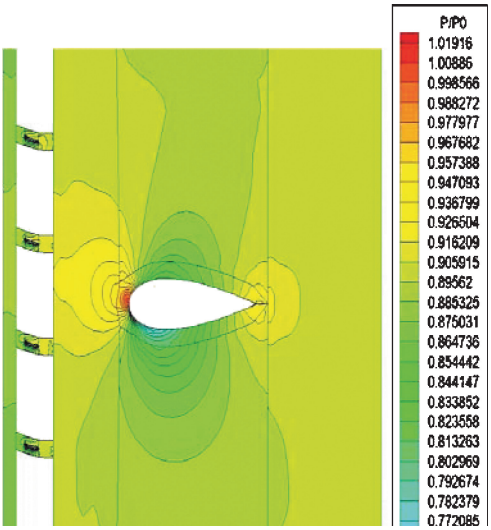

b) Static-pressure contours

Fig. 6 OGV–pylon coupled solution [five passages (two harmonics) retained in OGV region].

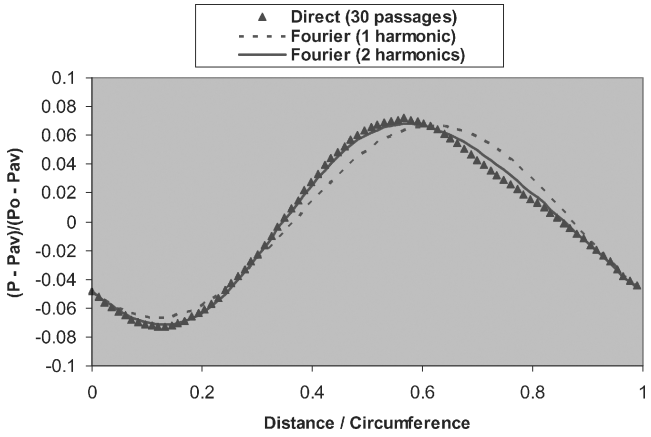

Fig. 7 Static-pressure distributions along circumference (at OGV inlet).

solution. The results demonstrate a very fast and desirable harmonic convergence.

In general, the reduction factor in computational mesh points in the circumferential direction in comparison with a direct whole annulus solution is given by

$$\frac{2\pi}{(2N+1)\Delta\theta} \tag{5}$$

where $\Delta\theta$ is the circumferential spacing (in radians) of the basic truncated domain and N is the number of harmonics retained. For a duct field without blades, the basic truncated domain contains only one mesh cell, and the mesh reduction factor is thus

$$\frac{\text{total circumferential mesh cells of direct solution}}{(2N+1)} \tag{6}$$

On the other hand, for a bladed region $\Delta\theta$ is the blade passage pitch; hence, the corresponding mesh reduction factor is

$$\frac{\text{total number of blade passages in direct solution}}{(2N+1)} \tag{7}$$

In terms of the time-marching convergence rate, the Fourier solutions have typically been shown to converge faster than direct solutions. This might well be attributed to the fact that the Fourier transform effectively enables an instantaneous circumferential communication throughout the whole domain at each step. The communication between the two circumferential boundaries will have to take at least a few steps in a full-domain direct solution with an explicit solver. The overhead caused by the Fourier transform is about 40–50% for a duct domain, where every mesh cell will be involved. For a bladed domain, the Fourier transform only needs to be carried out at the blade passage boundaries. Hence the overhead can be within 5–10%, depending on the mesh density. More specifically, for the three-dimensional intake duct under a crosswind, the mesh points are reduced by a factor of 27 when five harmonics are used. The saving in CPU is by a factor of about 20. For the OGV-pylon interaction case, the mesh points are reduced by a factor of six, and the saving in CPU is about of factor about five, when two harmonics are included.

III. Modeling of Nonaxisymmetrical Unsteady Flow

A. Modeling Consideration and Formulation

In general, an unsteady flow variable can be expressed in terms of a time-averaged base and an unsteady fluctuation:

$$\tilde{U}(x,r,\theta,t) = U(x,r,\theta) + U'(x,r,\theta,t) \tag{8}$$

Assume the unsteady disturbance is a linear perturbation from a steady state. A kind of problem of interest is the propagation of acoustical pressure waves of small magnitude in a nonaxisymmetrical base flowfield. Then we can deal with each temporal harmonic

separately. A harmonic perturbation in time at a frequency ω can be expressed by a pair of complex conjugates:

$$\tilde{U}(x,r,\theta,t) = U(x,r,\theta) + \hat{U}_1(x,r,\theta)e^{i\omega t} + \hat{U}_{-1}(x,r,\theta)e^{-i\omega t} \tag{9}$$

where $\hat{U}_1 = U_r + iU_i$ and $\hat{U}_{-1} = U_r - iU_i$. Hence, the unsteady flow can be fully determined if we know the steady base flow $U(x,r,\theta)$ and the real and imaginary parts of the complex amplitude (mode shape) Ur, Ui.

The steady nonaxisymmetrical base flow can be obtained efficiently as described in the preceding section. Noting that Ur and Ui are space dependent only; therefore, we can also express their circumferential variations in terms of an Nth-order spatial Fourier series with respect to θ, similar to Eq. (1):

$$U_r(x,r,\theta) = \bar{U}_r(x,r) + \sum_{n=1}^{N}\left[(A_r)_n\sin(n\theta) + (B_r)_n\cos(n\theta)\right] \tag{10a}$$

$$U_i(x,r,\theta) = \bar{U}_i(x,r) + \sum_{n=1}^{N}\left[(A_i)_n\sin(n\theta) + (B_i)_n\cos(n\theta)\right] \tag{10b}$$

In this way, we now use the circumferential Fourier series to approximate the equivalent mode shape of the unsteady perturbations. A relevant issue is how many circumferential points we now need to do the Fourier transform to capture a typical mode shape of practical interest. For instance, consider an axisymmentrical intake duct where unsteadiness is generated by a downstream fan with 25 blades. The corresponding rotating harmonic unsteadiness at the blade-passing frequency ω will be in a form of

$$U'(x,r,\theta,t) = A(x,r)\sin(\omega t + N_d\theta) \tag{11}$$

where N_d is the number of nodal diameters of the circumferentially traveling wave mode, and in this case equals to the number of fan blades, and $A(x,r)$ is a positive real number. It can be shown that corresponding real and imaginary parts [Eqs. (9) and (10)] vary circumferentially in a sinusoidal manner:

$$U_r(x,r,\theta) = C(x,r)\cos(N_d\theta) \tag{12a}$$

$$U_i(x,r,\theta) = C(x,r)\sin(N_d\theta) \tag{12b}$$

where $C(x,r)$ is a real number. For the present case ($N_d = 25$), a straightforward Fourier representation of the mode shape would be required at least to retain 25 circumferential harmonics to capture the circumferential variation of the unsteadiness. On the other hand, however, we already know the circumferential traveling wave speed (fan rotation speed) and the number of nodal diameters (fan blade number). Thus, the relative temporal phase angle of the unsteadiness between any two points for a given (x,r) is fixed. Hence the only unknown is the amplitude, that is, the mode shape is independent of θ. This can be easily seen by phase shifting back the unsteadiness at θ [Eq. (11)] by $N_d\theta$. The phase-shifted unsteadiness is clearly independent of θ. Practically only one circumferential mesh cell would be needed in the solution, and the whole circumferential domain can be constructed by the known phase relation.

The preceding consideration for an undistorted axisymmetric flow is now extended to a distorted nonaxisymmetric one. Consider a case where the amplitude of the unsteady harmonic caused by the rotating fan blades is modulated by an inlet distortion of a wavelength of the whole annulus. The real and imaginary parts are assumed to be in form of

$$U_r(x,r,\theta) = C(x,r)\sin(\theta)\cos(N_d\theta) \tag{13a}$$

$$U_i(x,r,\theta) = C(x,r)\sin(\theta)\sin(N_d\theta) \tag{13b}$$

To capture the unsteady flowfield, we only need to know how the mode shape is distorted circumferentially. Instead of using the complex amplitude $\hat{U}_1$ directly, we use a phase-shifted one $\hat{U}_1 e^{-iN_d\theta}$, which should only have a long wavelength circumferential variation corresponding to the distortion. As a result, the circumferential mesh points required for the Fourier solution can be significantly reduced. Denote $\hat{U}_1' = \hat{U}_1 e^{-iN_d\theta} = U_r' + iU_i'$. The circumferential Fourier transform is then carried out with respect to the phase-shifted complex amplitude $\hat{U}_1'$ (e.g., for the nth spatial harmonic of its real part):

$$(A_r')_n = \frac{2}{2N+1}\sum_{1}^{2N+1}\text{Real}(\hat{U}_1')\sin(n\theta) \tag{14a}$$

$$(B_r')_n = \frac{2}{2N+1}\sum_{1}^{2N+1}\text{Real}(\hat{U}_1')\cos(n\theta) \qquad (n = 1, 2, \ldots, N) \tag{14b}$$

After the circumferential representations of the real and imaginary parts of $\hat{U}_1'$ are obtained from the Fourier series, the complex amplitude at any circumferential position θ is given by $\hat{U}_1 = \hat{U}_1' e^{iN_d\theta}$.

By using the preceding technique, we effectively use the Fourier series to model the deviation of a distorted traveling wave from an undistorted one. Consequently, the same number of circumferential Fourier harmonics can be used for both the distorted steady baseflow and unsteady perturbations. The rest of the method follows more or less the same procedure as that for a steady flow.

B. Computational Example

A two-dimensional intake duct section of a constant radius is used. The intake is subject to an inlet stagnation pressure circumferential distortion with an amplitude of 30% dynamic head. At the exit, the duct is subject to upstream running acoustic waves to simulate a rotating unsteady pressure field generated by a transonic fan rotor. The amplitude of the unsteady pressure at the exit is specified to be 500 Pa. It is assumed that the rotor of 20 blades rotates at a tangential velocity of 418 m/s. Consider the fundamental temporal harmonic at the blade passing frequency. Again, the validation of the new method is made by comparison with a direct solution of the time-linearized equations over the full 360-deg domain. Numerical tests showed that for the present second-order spatial discretization at least 20 mesh points should be needed for accurately resolving one harmonic. In this case, 30 circumferential mesh cells are taken nominally to resolve one spatial harmonic. Hence, for the whole annulus domain covering 20 harmonics, 600 mesh cells are used in the direct calculation. For the Fourier solution on the other hand, five harmonics are retained, so that only 11 circumferential cells are needed in the calculation. Thus we have a drastic reduction of mesh cells by a factor of nearly 55 times.

The distorted steady flow pattern and the comparison between the Fourier solution and the direct solution are similar to those as shown in Fig. 3. Figure 8a shows the instantaneous static-pressure contours reconstructed from the Fourier solution. Figure 8b shows the result from the direct solution using the whole annulus domain. The upstream propagated pressure waves are clearly distorted by the nonuniform steady base flow, and this distortion effect is accurately captured by the Fourier-transform-based solution, which uses only 2% of the mesh points. The saving in CPU achieved in this case is only about a factor of 11. This is largely because of the extra computing time required by the Fourier transform. Further speed up is expected with efforts in optimized coding for complex variables. A more quantitative comparison is given in Fig. 9 for the circumferential distributions of instantaneous pressures at an axial position 50% of the duct length. The excellent agreement between the two solutions clearly demonstrates the validity of the present Fourier-transform-based approach. The present method offers a significant advantage for efficient and accurate solutions to the time-linearized flow equations for blade tone noise propagations in nonaxisymmetric duct flows.

Similar to the steady flow example for an OGV-pylon interaction, the present method can also be applied to the circumferential "aperiodic" steady and unsteady flows in blade rows, where the passage-to-passage aperiodicity is either caused by relatively stationary

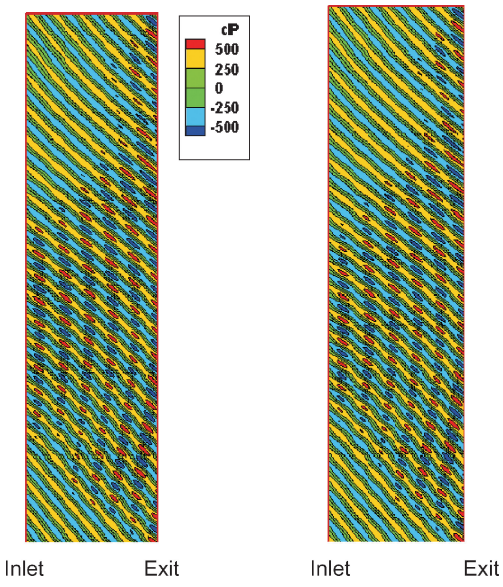

a) Fourier solution **b) Direct solution**

Fig. 8 Instantaneous static-pressure contours (inlet stagnation pressure distortion with wavelength 2π; upstream running acoustic waves at exit with wavelength of $2\pi/20$).

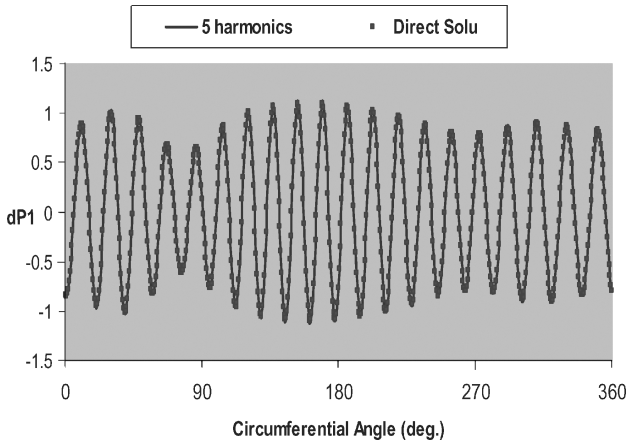

Fig. 9 Circumferential distributions of instantaneous static pressure at middomain (inlet stagnation pressure distortion with wavelength 2π; upstream running acoustic waves at exit with wavelength of $2\pi/20$).

inlet/exit distortions (e.g., inlet distortion/compressor inlet-guide-vane interaction) or by rotor-rotor (or stator-stator) interactions.

IV. Conclusions

In recent years, the Fourier-transform-based approach has been developed in various forms for efficient computations of unsteady turbomachinery flows. Previous work was limited to flows in blade rows subject to a phase-shift periodicity. The present work extends the capability to dealing with nonaxisymmetric steady and unsteady flows. The modeling formulations and computational sample cases are presented for a nonaxisymmetric duct flow under a crosswind and acoustic propagation of pressure waves in a distorted flow. Comparisons of the present Fourier solutions against the whole annulus calculations confirm the validity of the methodology. It is clearly demonstrated that the approach is accurate and effective, leading to a significant computational speed up (10–30 times for the cases studied) over a direct whole annulus solution.

References

[1]He, L., "An Euler Solution for Unsteady Flows Around Oscillating Blades," *Journal of Turbomachinery*, Vol. 112, No. 4, 1990, pp. 714–722.

[2]Dewhurst, S., and He, L., "Unsteady Flow Calculations Through Turbomachinery Stages Using Single-Passage Domain with Shape-Correction Method," *Proceedings of the 9th International Symposium on Unsteady Aerodynamics and Aeroelasticity in Turbomachines*, edited by P. Ferrand and S. Aubert, Press Univ. de Grenoble, Grenoble, France, 2000, pp. 338–350.

[3]Gerolymos, G. A., Michon, G. J., and Neubauer, J., "Analysis and Application of Chorochronic Periodicity in Turbomachinery Rotor/Stator Interaction Computations," *Journal of Propulsion and Power*, Vol. 18, No. 6, 2002, pp. 1139–1152.

[4]Li, H. D., and He, L., "Blade Aerodynamic Damping Variation with Rotor-Stator Gap-A Computational Study Using Single-Passage Approach," *Journal of Turbomachinery*, Vol. 127, No. 3, 2005, pp. 573–579.

[5]Li, H. D., and He, L., "Single-Passage Analysis of Unsteady Flows Around Vibrating Blades of a Transonic Fan Under Inlet Distortion," *Journal of Turbomachinery*, Vol. 124, No. 2, 2002, pp. 285–292.

[6]Schnell, R., "Investigation of the Tonal Acoustic Field of a Transonic Fan Stage by Time-Domain CFD Calculations with Arbitrary Blade Counts," American Society of Mechanical Engineering, Paper GT-2004-54216, June 2004.

[7]Hall, K. C., Thomas, J., and Clark, W. S., "Computation of Unsteady Nonlinear Flows in Cascades Using a Harmonic Balance Technique," *AIAA Journal*, Vol. 40, No. 5, 2002, pp. 879–886.

[8]McMullen, M. S., Jameson, A., and Alonso, J., "Application of a Non-Linear Frequency-Domain Solver to the Euler and Navier–Stokes Equations," AIAA Paper 2002-0120, Jan. 2002.

[9]Shrinivas, G. N., and Giles, M. B., "OGV Tailoring to Alleviate Pylon-OGV-Fan Interaction," American Society of Mechanical Engineers, Paper, 95-GT-198, June 1995.